Supporting Information

Z-type heterojunction degradation of tetracycline by 2D g-C_3N_4 with 3D oxygen vacancy Bi_2WO_6

*Xiao Kang, Xiangyan Li, Abulikemu Abulizi, Mihiriguli Abulimiti, Nuerla Ailijiang, Anwar Mamat**

* Corresponding author

Xiao Kang, Xiangyan Li, Abulikemu Abulizi, Mihiriguli Abulimiti, Anwar Mamat

State Key Laboratory of Chemistry and Utilization of Carbon Based Energy Resources, Key Laboratory of Oil & Gas Fine Chemicals, Ministry of Education & Xinjiang Uyghur Autonomous Region, School of Chemical Engineering and Technology, Xinjiang University, Urumqi 830017, P.R. China.

E-mail: anwarm@xju.edu.cn https://orcid.org/0009-0006-0387-1612

Nuerla Ailijiang

Key Laboratory of Oasis Ecology of Education Ministry, College of Ecology and Environment, Xinjiang University, Urumqi 830017, P.R. China.

Text S1 Materials

Melamine ($C_3H_6N_6$) was purchased from Shanghai Shanpu Chemical Co. Bismuth nitrate ($Bi(NO)_3$-$5H_2O$) was purchased from Shanghai McLean Biochemical Technology Co. Sodium tungstate ($NaWO_4$-$2H_2O$) was purchased from Tianjin Xinbute Chemical Co. CTAB ($C_{19}H_{42}BrN$) and ammonia (NH_3-H_2O) were purchased from Tianjin Zhiyuan Chemical Reagent Co. Sulfuric acid (H_2SO_4), methanol (CH_3-OH), sulfuric acid (H_2SO_4), and nitric acid (HNO_3) were purchased from Sichuan Xilong Science Co.

Text S2 Characterizations

The physical phases and compositions of the samples were characterized by powder X-ray diffraction (XRD, Rigaku, Japan), the chemical structures of the samples were analyzed by Fourier transform infrared spectroscopy (FT-IR), the morphologies of the photocatalysts were further investigated by emission scanning electron microscopy, and the surface elemental compositions of the photocatalysts were determined by energy dispersive X-ray spectroscopy (EDS). For further morphological and structural evaluation, the chemical composition and valence states of the photocatalysts were determined by X-ray photoelectron spectroscopy (XPS, Thermo Fisher Scientific), the exact surface area of the photocatalysts was determined by Brunauer–Emmet–Teller (BET, Autosorb-iQ), and the surface area of the photocatalysts was determined by UV–VIS diffuse reflectance spectroscopy (UV–Vis). UV–Vis Diffuse Reflectance spectroscopy (UV–Vis DRS, Jasco) was used to detect the absorption wavelengths of the photocatalysts and calculate their band gap energies. Steady-state and transient fluorescence tests were conducted on an Edinburgh FLS1000 instrument in the United Kingdom, while electron paramagnetic resonance (EPR) tests were conducted on a Bruker EMXplus-6/1 instrument in Germany.

Text S3 Photoelectrochemical measurements

Photoelectrochemical measurements of the prepared samples were conducted on a CHI 660E Electrochemical Workstation equipped with a conventional three-electrode electrochemical system. The as-prepared samples were deposited on ITO (0.5 × 1.5 cm) to serve as the working electrode. A Pt wire was used as the counter electrode, while an Ag/AgCl electrode was used as the reference electrode. A Na_2SO_4 solution (0.5 M) was used as the electrolyte. The working electrodes were prepared via the following method: 5 mg obtained catalyst sample, previously dissolved in 1 mL ethanol with 10 μL Nafion, was dropped to disperse uniformly on the ITO glass. Subsequently, the photocatalyst-coated ITO glass was annealed for 10 h in a drying oven at 80 °C.

Table R1 Catalyst properties for degrading pollutants.

Materials	Catalyst	Degradable material	Degradation efficiency	Reference
$g\text{-}C_3N_4$	$g\text{-}C_3N_4/Bi_2O_3$	THM	84.6%	[1]
	$g\text{-}C_3N_4/Bi_2MoO_6$	Estradiol	96%	[2]
	$\alpha\text{-}Fe_2O_3/g\text{-}C_3N_4$	MB	88%	[3]
	$\alpha\text{-}Fe_2O_3/g\text{-}C_3N_4$	MO	38%	[3]
	$\alpha\text{-}Fe_2O_3/g\text{-}C_3N_4$	Phenol	60%	[3]
Others	ZnO (CuNi-ZnO)	IC	93.32%	[4]
	CeO/ZnO	TC	95.9%	[5]
	$Cu_2V_2O_7/\alpha\text{-}Fe_2O_3$	MB	88%	[6]
	WO_3/AgI	CTC	88.1%	[7]

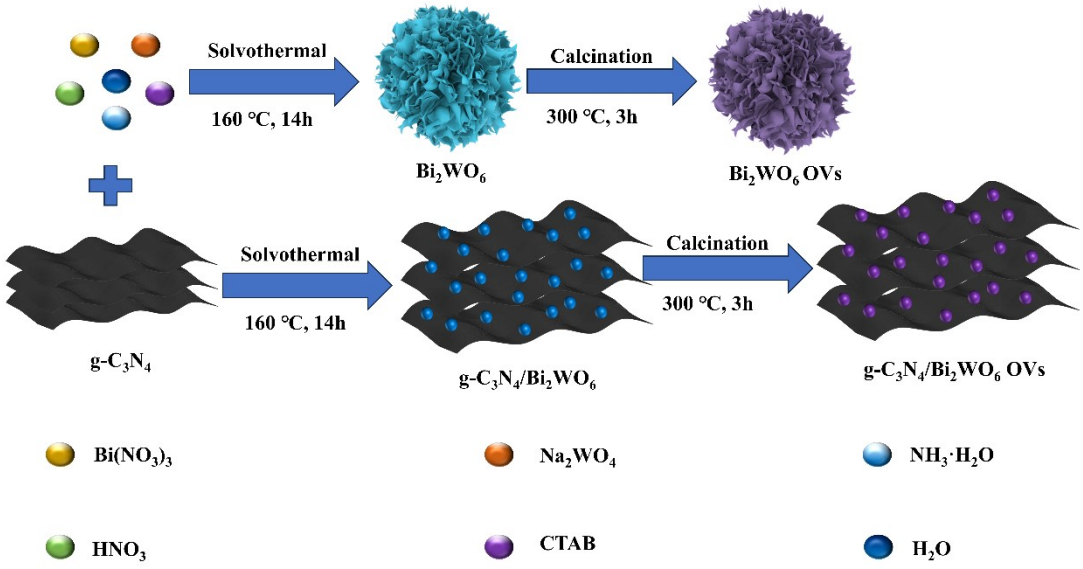

Fig. S1. The preparation process of BWO and CN/BWO OVs catalysts

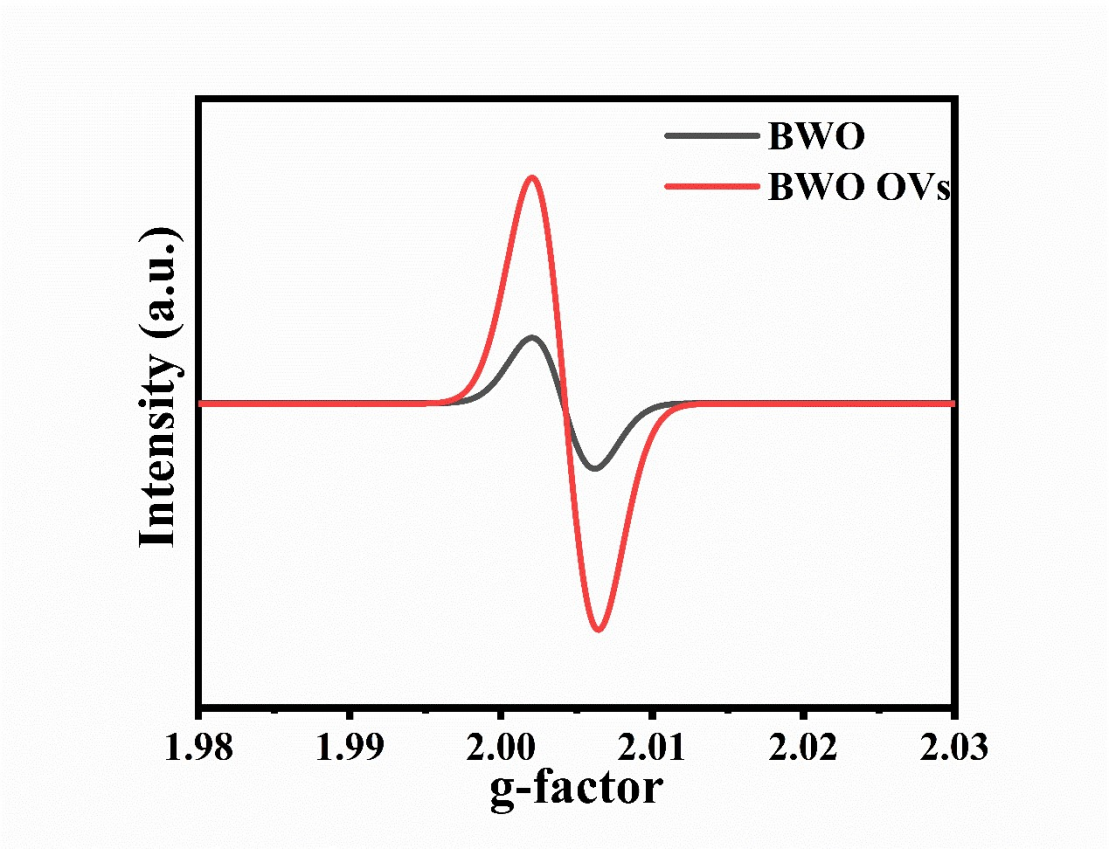

Fig. S2. ESR spectra of pure Bi_2WO_6 and Bi_2WO_6 OVs.

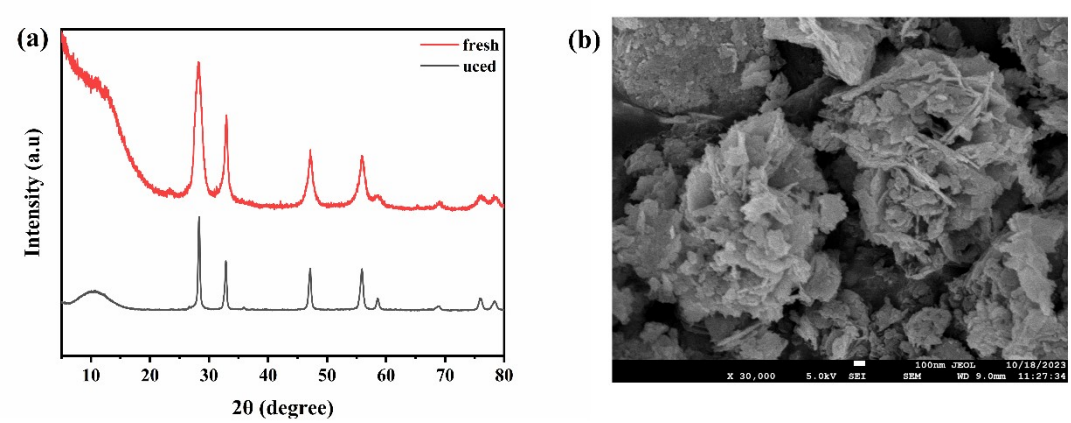

Fig. S3. XRD images of CN/BWO OVS 30% catalyst before and after reaction (a), and the SEM image of CN/BWO OVs30% catalyst after reaction (b).

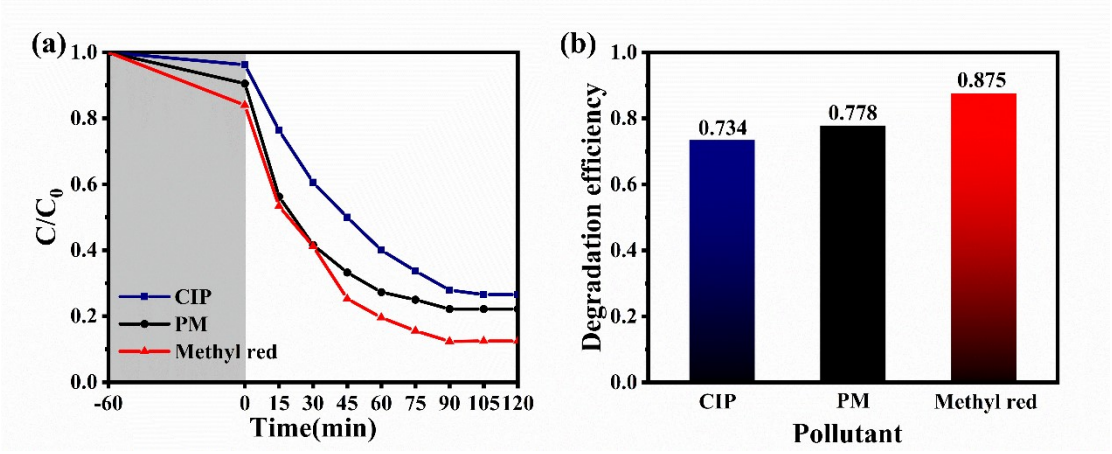

Fig. S4. Degradation of other pollutants

References

1. *Chemical Engineering Journal*, 2024, **499**.
2. Z. F. Lin, H. Y. Lin, R. A. Doong and A. I. Schfer, *Journal of Hazardous Materials*, 2024, **476**.
3. K. Kalantarian and S. Sheibani, *Ceramics International*, 2024, DOI: 10.1016/j.ceramint.2024.08.127.
4. R. Kumar and R. S. Gedam, *Ceramics International*, 2024, DOI: 10.1016/j.ceramint.2024.04.208.
5. J. Huang, M. Lu, P. Wei, Y. Xie, H. Xie, M. Liu, L. Li, J. Hu, Z. Zhang and Y. Qi, *Journal of Environmental Chemical Engineering*, 2024, DOI: 10.1016/j.jece.2024.113074.
6. F. Li, X. Li, S. Tong, J. Wu, T. Zhou, Y. Liu and J. Zhang, *Nano Energy*, 2023, DOI: 10.1016/j.nanoen.2023.108849.
7. C. Wang, X. Li, X. Lv, X. Huang, Y. Zhao, T. Deng, J. Zhang, J. Wan, Y. Zhen and T. Wang, *Journal of Cleaner Production*, 2024.